FUNDAMENTAL RESEARCH

For. Sci. 65(4):496–507
doi:10.1093/forsci/fxz006
Published by Oxford University Press on behalf of the Society of American Foresters 2019.

forest management

Lowering Stand Density Enhances Resiliency of Ponderosa Pine Forests to Disturbances and Climate Change

Jianwei Zhang, Kaelyn A. Finley, Nels G. Johnson, and Martin W. Ritchie

Stand density affects not only structure and growth, but also the health of forests and, subsequently, the functions of forest ecosystems. Here, we integrated dendrochronology and repeated inventories for ponderosa pine research plots to determine whether long-term growth and mortality responded to climate trends and how varying stand density influenced the responses. The plots were established prior to 1975 on existing stands throughout northern California. Although annual temperature increased consistently for the last 65 years, ring-width indices produced by eliminating age and thinning effects failed to detect radial trend regardless of site quality. However, interannual variation for the indices was substantial, reflecting a strong influence of climate on tree growth. Plot-level basal area increments were significantly affected by tree mortality. Stand density index explained most variation of mortality. Lowering stand density enhanced remaining tree growth, reduced mortality, and increased stand resiliency to disturbances and climate change. Besides higher climate moisture indices or lower vapor pressure deficits, any treatments that improve tree vigor and reduce stress will have a similar effect to reducing stand density. Although neither biotic disturbances nor abiotic conditions can be controlled, forest managers can manage stand density appropriately to enhance resilience to climate change and disturbances.

Keywords: Stand Density Index, long-term research plots, dendrochronology, *Pinus ponderosa*, bark beetle disturbances

Driven by economic and population growth, increases in wildfire frequency and intensity, insect and disease outbreaks, and the loss and addition of species, the world's forest ecosystems have been greatly changed in structure and functions (Vitousek et al. 1997, Lugo 2015, Trumbore et al. 2015). Climate has played a prominent role in driving these changes by altering disturbance regimes and forest growth (Westerling et al. 2006, Seidl et al. 2017). Although climate constantly changes, the planet is warmer today than it has been for thousands of years (IPCC 2014). An increase in atmospheric carbon dioxide has contributed to the warming trend. Long-lived forest trees have recorded these changes over their life spans. Because the majority of tree mass is made from carbon dioxide assimilated from the atmosphere through photosynthesis, the climate signatures and any other disturbances recorded in their annual tree-rings provide us with an opportunity to explore how trees respond to climate (Fritts and Swetnam 1989). In return, forests also influence climate by adjusting atmospheric CO_2, water cycling, and solar radiation (Bonan 2008). Therefore, dendrochronological data not only relate to contemporary climate, but also quantitatively provide tree growth or carbon accumulation.

A forest consists of many individual trees and other associated organisms that interact with one another. Using tree rings to study forest growth and carbon sequestration faces some shortcomings because collecting tree cores from all trees in a stand is a challenge. Although we can potentially collect them all in a forest stand, this has rarely been done, and we miss trees that died in the past, particularly in areas with fast decomposition rates. Although dendrochronology has been reliably used to identify periods of mortality indicated by a release in surviving tree radial growth, it will not provide an accurate number for tree mortality. Without estimates

Manuscript received July 30, 2018; accepted November 2, 2018; published online March 30, 2019.

Affiliations: *Jianwei Zhang (jianweizhang@fs.fed.us), Kaelyn A. Finley (kaelynfinley@fs.fed.us), and Martin W. Ritchie (mritchie@fs.fed.us), USDA Forest Service, Pacific Southwest Research Station, 3644 Avtech Parkway, Redding, CA 96002. Nels G. Johnson (nelsjohnson@fs.fed.us), USDA Forest Service, Pacific Southwest Research Station, 800 Buchanan Street, Albany, CA 94710.*

Acknowledgments: *A long-term study of such magnitude would not be possible without the dedication of people who designed, installed, maintained, and measured these research plots for more than a half century. We sincerely thank them all, especially our colleague William Oliver who designed and oversaw the installation and early data collection. Thanks to many current and former supporting personnel in the Redding Lab, and many others in the National Forests who assisted with the study in various stages; the names are numerous, and each has our personal thanks. The comments from Associate Editor and two anonymous reviewers improved the manuscript and are greatly appreciated. Use of trade names in this paper does not constitute endorsement by the United States Forest Service.*

of tree mortality over time, stand growth dynamics are impossible to quantify accurately.

Permanent forest research plots with repeated measurements can overcome this pitfall. Long-term data collected from these plots quantify stand dynamics recorded over time because each individual tree has observations on its health, growth, and survival. No other method is capable of precisely quantifying biomass lost to mortality. However, the effect of climate on stand growth and health is difficult to construct from these datasets because (1) trees in the permanent plots were not annually measured, so the average climatic data over the measuring period may wash out extreme and/or isolated weather events, and (2) growth is confounded with tree age and other disturbances. Both limitations can be solved with dendrochronological analysis. Therefore, a study combining dendrochronological data and long-term measurements from permanent plots can explore the stand-level responses to climate change and other disturbances including stand density management by thinning, a standard forest practice to increase growth of residual trees. In recent years, this practice, sometimes in conjunction with prescribed fire, has been found to be an effective tool in promoting resilient ponderosa pine forests. For example, thinning has been widely recommended to mitigate climate change impacts on growth by increasing water availability and water-use efficiency (McDowell et al. 2003, 2006). Trees grown in lower-density plots are less vulnerable to drought events and more resistant to bark beetle attacks (Zhang et al. 2013b, c). Thus, thinning a stand reallocates water and other resources to residual trees and may provide a drought-adaptation tool that could potentially reduce adverse ecological and socioeconomic impacts of climate change (Sohn et al. 2013, 2016a, b). Furthermore, thinning is a key tool for fuel reduction, as managers are often reluctant to prescribe fire in a dense stand without first thinning. From the National Fire and Fire-Surrogate Study findings, Stephens et al. (2012) concluded that both prescribed fire and thinning successfully met the short-term fuel-reduction objectives such that the treated stands would be more resilient to high-intensity wildfire.

Over the past 100 years, scientists of the USDA Forest Service have established and measured research plots and other temporary plots across a range of densities. From temporary plot data, Reineke (1933) developed SDI, which is a measure of the stocking of a stand of trees based on the number of trees per unit area and quadratic mean diameter. Since then, many long-term research plots were established to examine the effect of stand density on growth and development for many tree species across United States. Here, we use long-term ponderosa pine (*Pinus ponderosa* Lawson & C. Lawson var. *ponderosa*) research plots in northern California, established and/or maintained by the Pacific Southwest Research Station in Redding, CA during the last 60 years to bridge long-term growth and health of forest stands with the effect of climate change during these study periods.

The specific objectives of this study are:

a) to address if tree growth responds to observed climatic variables such as temperature (maximum, minimum, and average), precipitation, and other derived metrics (potential evapotranspiration (PET), Climatic Moisture Index [CMI], etc.), by factoring out age-related radial growth decline and other disturbance effects including density manipulation through thinning or bark beetle outbreaks;

b) to determine stand-level annual basal area response to density by filling in annual radial growth for all trees in the plots that have been measured every 5 years since plot installations;

c) to evaluate the mortality relation with stand density and climate change;

d) to describe the trend differences across a range of site quality and possible interactions with thinning density or climate variables on stand growth and tree mortality.

Materials and Methods

Plot Selection

We selected 42 permanent research plots of ponderosa pine established between 1958 and 1972 at six sites with varying site quality in northern California (Table 1, Figure 1). Diameter at breast height (dbh) (1.37 m or 4.5 ft), mortality, and condition of trees in all plots have been measured multiple times since plot establishment. Measurements also included total height and height to base of live crown, either for all of or for a 20 percent sample of trees in the plot. Inventories typically occurred every 5 years after plot establishment. The plots were established in either natural, even-aged pure stands or mono-species plantations of ponderosa pine. The site index of these plots ranges from 21 m (70 ft) to 49 m (160 ft) (Meyer 1938) at 100 years (Table 1), based on the 75th percentile of plot height and total tree age (Ritchie et al. 2012). We selected sites where multiple plots were installed with a range of densities.

On our earliest study installation at Sugar Hill, the plantation was thinned to either 3*D*+4 foot or 2*D*+4 foot spacing, where *D* is the quadratic mean diameter in inches. For example, if *D* was 15.2 cm (6 in.), the stand was thinned to 6.7 m (22 ft) spacing between trees for the 3*D*+4 density treatment and 4.9 m (16 ft) spacing for the 2*D*+4 treatment. In both the Edson Creek and Show Plantation studies, density treatments were achieved by thinning stands to 40

Management and Policy Implications

Density management can improve forest growth and health by controlling growing stock, through initial spacing or subsequent thinning, which makes the limited soil water and nutrients available to the remaining trees. This long-standing forestry practice can also be integrated to achieve other management objectives such as more water production, better wildlife habitats, and reduced fuel loads. Results from this study suggest that lowering stand density for ponderosa pine stands enhanced remaining tree growth, reduced mortality, and increased stand resiliency to bark beetle disturbance and, to some extent, climate warming and drought. Although a density threshold varies with site quality, stand age when thinning applies, and rotation age, stands with a Stand Density Index (SDI) of more than 600 trees ha^{-1} (240 trees ac^{-1}) will exhibit reduced individual tree growth and a high probability of suffering from mortality in northern California. If resources permit, repeated density management is desirable, which not only produces maximum high-quality timber, but also has chance to manipulate stand structure and maximize their functions. Although neither climate nor disturbances can be easily controlled, forest managers can manage stand density based on stand age and environmental conditions to mitigate the threats from climate change and potential disturbances.

Table 1. Permanent research plot information and site characteristics for ponderosa pine from higher to lower latitudes in northern California, USA.

Location	No. of plots	Plot size (ha)	SI[a] (m)	Elevation (m)	Stand[b] history	Age span	ΔT_{65}[c] (°C) (T_{max}/T_{min})	No. of tree cores	Density regimes
Sugar Hill	3	0.40	25–31	1,646	P	27–85	–0.5/1.4	29	3
Edson Creek	3	0.40	39–43	1,190	N	87–131	1.4/0.7	26	3
Show Plantation	3	0.40	40–45	1,189	P	53–97	1.4/0.9	27	3
Prattville	3	0.20	34–37	1,433	P	15–60	0.5/3.5	47	3
Trough Springs	18	0.03	21–24	1,280	P	11–57	0.9/1.8	121	2
Elliot Ranch	15	0.20	44–49	1,183	P	20–65	1.2/1.8	60	5

Note: [a]SI, site index at 100 years; [b]N, natural stand, P, plantation; [c]ΔT_{65}, temperature change estimated from temperature–year regression lines (Figure S1) during the last 65 years (1950–2015).

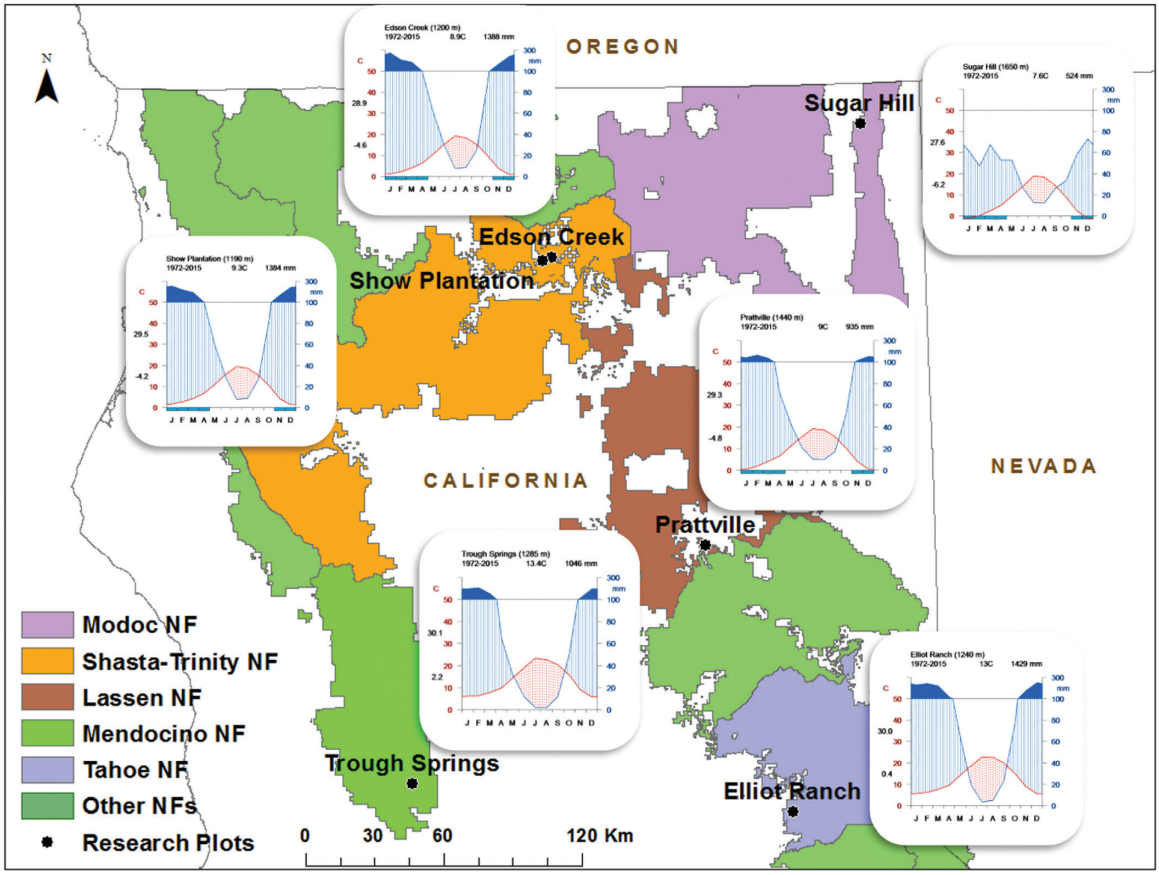

Figure 1. Site locations and Walter's climate diagram for each sites of ponderosa pine long-term permanent plots across northern California.

percent, 55 percent, and 70 percent of the maximum basal area at full occupancy based on Meyer's yield table (1938). The densities at Trough Springs were originally established with planting at four square spacings of 2.1, 2.4, 3.0, and 4.3 m (7, 8, 10, and 14 ft) and an unthinned control, with three plots per spacing (Zhang et al. 2006). Each plot was split into three subplots with a complete understory vegetation removal (V0), half removal (V0.5), and no removal (V1). Later, similarities between the control and 2.1 m (7 ft) spacing led to the decision to combine these treatments, and subsequently both were considered the control spacing. In this paper, we only include the lowest density (4.3 m or 14 ft spacing) and control plots, both with the three understory vegetation removal treatments. The Elliot Ranch plots were installed with growing stock levels of 9, 16, 23, 30, and 37 m^2 ha^{-1} (40, 70, 100, 130, and 160 ft^2 ac^{-1}, respectively) (Zhang et al. 2013b). At Prattville, plots were installed in the existing stands with or without precommercial thinning with three plots being 250, 960, and 1,070 trees ha^{-1} (100, 390, and 430 trees ac^{-1}). Here, we kept the original terms of treatment for all study locations to only reflect the contemporary forest practice, which will not affect our analysis because we use SDI as the independent variable for the sake of site comparisons.

Increment Core Collection

Within each permanent plot or subplot, at least four live trees per diameter class were randomly selected from three diameter size classes, and an increment core was collected from breast height (4.5 ft or 1.37 m) (Table 1). An additional increment core was

collected from stump height (12 in. or 30 cm) from a subset of the sample trees. A total of 318 tree cores were collected, and 310 of them were included for the analysis.

Tree-Core Processing Procedure

In the lab, the increment cores were dried, mounted, sanded, and cross-dated using standard dendrochronological methods (Stokes and Smiley 1996, Speer 2010). Twisted cores were straightened using the steam method (Speer 2010). Cores were visually cross-dated using the list method by comparing within the individual density treatments at each study location (Yamaguchi 1991). Ring widths were then measured to 0.001 mm accuracy using either a scanned image (1,200 dpi) in CooRecorder or a stage micrometer using the Velmex measuring system (Velmex, Bloomfield, NY). The program COFECHA was used to statistically assess the quality of the visual cross-dating (Grissino-Mayer 2001). Cores with dating issues identified by COFECHA were re-examined, and any distinguishable errors were corrected. Eight cores that could not be reliably assigned calendar dates were not included in further analysis, leaving 310 cores. In order to remove undesirable disturbance and age-related trends in the series, chronologies were developed for each treatment/site using the program ARSTAN to convert raw ring-width measurements into a dimensionless ring-width index. Each location/treatment was standardized separately using a cubic smoothing spline two-thirds (67 percent) the series length with a 50 percent frequency cutoff. Tree-ring indices were calculated as ratios, and series were averaged together using robust (biweight) means (Cook 1985, Cook and Holmes 1999). ARSTAN produces three mean chronologies of the detrended series: the standard (STD) chronology, in which the detrended series are averaged together and autocorrelation is retained; the residual (RES) chronology, where autoregressive modeling is used to remove autocorrelation; and the ARSTAN (ARS) chronology, which reincorporates the autoregression patterns common to a majority of the individual series back into the final chronology (Cook and Holmes 1999, Baker et al. 2008). The RES chronology produced by ARSTAN was used for further analysis.

Several descriptive statistics commonly used in dendrochronology were used to compare the residual treatment chronologies produced in ARSTAN at each site for the time periods specified in Table 2. These included the standard deviation (SD), which estimates the variability of measurements for the whole series; mean RBAR, which is a measure of the common variance between the single series in a chronology and series intercorrelation, which is a measure of the strength of the signal (typically the climate signal) common to all sampled trees at the site; first-order autocorrelation (AC [1]) to detect persistence retained after the autoregressive model; and the expressed population signal (EPS).

EPS is a statistic introduced original by Wigley et al. (1984) that approximates how well a subsample represents an infinite population (Buras, 2017). EPS values depend on sample size and indicate whether chronologies are dominated by individual tree signals or stand-level (population) signals (Schwab et al. 2018). It is important to note that whereas many previous papers have used an EPS value of 0.85 or higher as an indicator of suitability for climate reconstructions, this threshold was arbitrarily chosen and does not necessarily reflect the strength of the climatic signal (Buras 2017).

Climate Data

Weather data were obtained from the PRISM climate group at Oregon State University, which triangulates data from multiple weather stations and accounts for geographical and topographical variations in order to give site-specific weather records dating back to 1895 (Daly et al. 2008). These weather data include

Table 2. Descriptive statistics of tree-ring chronologies within the optimum time span and regression equations with detrended residual chronologies as dependent variable and derived climate variables as the independent variables and adjusted r^2 for ponderosa pine grown at various locations in northern California.

Site	Time span	Treatment	rbar	SD	AC(1)	EPS	Regression equation	Adj-r^2
Sugar Hill	1946–2015	3*D*+4	0.49	0.10	0.09	0.85	0.80 + 0.30 CMI*	0.13
		2D+4	0.53	0.10	0.05	0.90	0.71 + 0.43 CMI*	0.21
		Control	0.45	0.11	–0.08	0.88	0.56 + 0.65 CMI*	0.37
Edson Creek	1917–2015	40%BA	0.37	0.11	0.05	0.78	1.52 – 0.02 VPD*	0.09
		55%BA	0.34	0.10	–0.07	0.80	1.49 – 0.02 VPD*	0.08
		70%BA	0.39	0.10	0.01	0.85	1.48 – 0.02 VPD*	0.07
Show Plantation	1944–2015	40%BA	0.39	0.12	0.22	0.82	1.36 – 0.01 VPD	0.02
		55%BA	0.20	0.14	0.17	0.72	1.33 – 0.01 VPD	0.05
		70%BA	0.32	0.12	0.25	0.81	1.56 – 0.02 VPD*	0.08
Prattville	1970–2016	LD	0.38	0.11	0.03	0.87	0.92 + 0.08 CMI*	0.08
		HD1	0.47	0.14	0.16	0.92	0.75 + 0.24 CMI*	0.37
		HD2	0.40	0.14	0.17	0.92	0.87 + 0.12 CMI*	0.10
Trough Springs	1969–2015	LD_V1	0.38	0.13	–0.06	0.92	0.76 + 0.21 CMI*	0.23
		LD_V0.5	0.43	0.14	0.11	0.92	0.78 + 0.19 CMI*	0.19
		LD_V0	0.47	0.13	0.07	0.88	0.87 + 0.10 CMI	0.05
		HD_V1	0.37	0.17	0.15	0.92	0.81 + 0.17 CMI*	0.10
		HD_V0.5	0.40	0.17	0.13	0.90	0.83 + 0.15 CMI*	0.13
		HD_V0	0.33	0.19	0.25	0.86	0.87 + 0.11 CMI*	0.09
Elliot Ranch	1966–2016	GSL40	0.41	0.12	0.07	0.86	0.51 + 0.09 CMI* + 0.08 GDD	0.10
		GSL70	0.42	0.12	0.08	0.89	0.30 + 0.14 CMI* + 0.11 GDD	0.23
		GSL100	0.39	0.13	0.00	0.89	0.13 + 0.12 CMI* + 0.15 GDD*	0.17
		GSL130	0.36	0.11	0.02	0.85	0.26 + 0.15 CMI* + 0.11 GDD*	0.25
		GSL160	0.38	0.13	0.02	0.88	0.16 + 0.12 CMI* + 0.15 GDD*	0.18

Note: AC(1), first-order autocorrelation; CMI, Climatic Moisture Index; EPS, expressed population signal; GDD, growing degree day; rbar, all series intercorrelation; SD, standard deviation for all cores; VPD, vapor pressure deficit. *$P < .05$ for testing $\beta_i = 0$.

precipitation (mm), average, minimum, and maximum temperature (°C) on a monthly scale. Derived variables also from the website are maximum and minimum vapor pressure deficit (VPD, hPa). All the weather variables used in this study will hereafter be referred to as climate variables because all analysis was done over decades, looking at long-term responses. Using these data, we calculated annual precipitation (PPT) from October of the previous year to the end of September in the current year, which presumably supports the current year growth. Similarly, we calculated annual potential evapotranspiration (PET, mm). A modified CMI from Willmott and Feddema (1992) was calculated as a ratio between PPT and PET during the same period time. We only averaged maximum VPD, minimum VPD, and minimum temperature from April to September as growing season VPD and T_{min}. Growing degree day above zero (GDD) was calculated by summing the mean temperature multiplied by the number of days in that month if the minimum temperature was greater than zero. The typical Mediterranean climatic patterns are shown for these sites in Figure 1.

Annual Basal Area and Mortality

Since the establishment of each study, all trees in a permanent plot were measured multiple times, usually every 5 years. We used the measured tree-ring radial growth averaged for each plot to interpolate annual dbh increment for all remaining trees during a particular period. Thus, we calculated the basal area for each tree per year, starting from the plot establishment year to the last time measured. All trees were measured in 2016 except for at Elliot Ranch, which was measured in 2014. Because a tree could have died any year during a measuring period, we estimated the year of mortality by interpolating the dbh from increment core trees compared with the live trees in the plot. For example, if the dbh of a dead tree was 17.5 cm (6.9 in.) in 1999 and was 16.7 cm (6.6 in.) in 1994, we calculated that the dbh increment was 0.8 cm (0.3 in.). In the mean time, if we found that an increment of mean dbh was 2.5 cm (1.0 in.) for all live trees in the plot during 1994–99 period, we would estimate that this tree died in 1996. For dead trees without a final dbh measurement, we used the tree-ring measurements from the trees from the same plot to estimate the year of mortality for that particular tree based on assumption that the dead tree would no longer be competing with its neighbor trees, so the neighbor trees would have grown proportionally more than the plot average. There might be some errors associated with the estimate for mortality in a particular year. Yet, this might be the best way to obtain annual mortality that would be better than an average over 5 years.

Data Analysis

1. After the tree-core data were detrended with a standardized method along the time series, an ordinary least-squares regression model was established for each density treatment at each site with the unitless detrended signal as the dependent variable (y_{dd}) and climate variables as the independent variables (x_i).

$$y_{dd} = \beta_i x_i + \varepsilon \tag{1}$$

The results address the first objective, determining if tree growth responded to climate variables. In particular, we want to see if climate change caused tree growth decline for the last 50 years, which is regarded as a period of dramatic change (IPCC 2014).

2. Using the annual dbh increment estimated for all trees since plots were established, we calculated the plot-level annual increment of basal area (BA, $m^2\ ha^{-1}\ year^{-1}$) and quadratic mean diameter (QMD, cm), trees per hectare (TPH), mortality (M, TPH), and SDI, Reineke 1933) with b being 1.77 (Oliver and Powers 1978).

$$\mathrm{SDI}_i = \mathrm{TPH}_i \left(\frac{\mathrm{QMD}_i}{25.4} \right)^b \tag{2}$$

3. A Bayesian approach is adopted (Gelman et al. 2013) for modeling tree mortality. The plots at Trough Springs were excluded because a sudden fire caused heavy mortality in 2012. We used the brm function in the brms package (Bürkner 2017) in R version 3.4.3 (R Core Team 2017) to fit a zero-inflated binomial generalized linear model with logit link function for both the binomial part and zero-inflated part (Hall 2000). The binomial model was chosen because in each year there is a fixed known number of trees that could die in each plot. If tree death is independent within year within plot, this model would be exactly binomially distributed. The zero-inflated model was chosen because 86 percent of observations experienced no tree mortality, which is substantially more than we would expect given a binomial model with the amount of mortality observed.

We considered three model scenarios of linear covariates for the binomial part of each model: SDI only, CMI only, and SDI and CMI together. Based on some preliminary graphical diagnostics, it was determined that the zero-inflated part of all models should contain only an intercept, as the presence of zeros did not appear to depend strongly on SDI, CMI, or plot ID. The full (scenario 3) zero-inflated model takes on the following form:

$$y_i \sim \begin{cases} 0, & \text{with probability } \phi \\ \text{Binonial}\,(N_i, p_i), & \text{with probability } 1-\phi \end{cases} \tag{3}$$

$$\log \frac{\phi}{1-\phi} = \beta_z \tag{4}$$

$$\log \frac{p_i}{1-p_i} = \beta_0 + \mathrm{SDI}_i \beta_{\mathrm{sdi}} + \mathrm{CMI}_i \beta_{\mathrm{cmi}} \tag{5}$$

where y_i is the number of dead trees in observation i, N_i is the number of live trees in i, ϕ is the zero-inflation probability defined in terms of log odds β_z, p_i is the probability of mortality of a single tree in i, β_0 is the associated intercept, β_{sdi} is the effect of SDI, and β_{cmi} is the effect of CMI.

Models were compared using the Leave One Out Information Criterion (Vehtari et al. 2016a, b), denoted LOO, using the LOO function in the brms package. The model with the lowest LOO is selected as the best model.

All prior distributions for the Bayesian analysis were set to the defaults provided by the brms package. The brm function calls Stan programming language (Stan Development Team 2017) to implement the Hamiltonian Monte Carlo algorithm (Duane et al. 1987, Hoffman and Gelman 2014) used to implement the

Bayesian analysis. For each scenario, we ran two 1,000 iteration chains each with a burn-in of 500. The adapt_delta parameter (see the brm function documentation for details) was set to 0.9999, and the maximum tree depth was set to 30 for all scenarios. All model parameters converged according to the Rhat diagnostic provided by the brm function.

When computing LOO, some observations had pareto_k (see LOO function documentation for details) values greater than 0.7 (five, three, and four observations for models 1, 2, and 3, respectively) and, as suggested by the software in this scenario, had to have their expected log predictive density recomputed without the assumption that these observations are negligible. This involved refitting the models for each problematic observation to compute the expected log predictive densities for the problematic observations directly.

Results

Climate Trends and Tree Ring Index

From 1950 to 2015, mean annual temperatures have increased at all sites (Figure S1), in which the minimum temperature (1.4 to 3.5°C) increased more than the maximum temperature (–0.5 to 1.2°C) at four sites (Table 1), whereas at Edson Creek and Show at the foothill of Mt. Shasta, the opposite trend was true. At Sugar Hill, a decreasing trend occurred for maximum temperature.

Among the three chronologies from the program ARSTAN, the RES was chosen for exploring climate signal in the tree rings. Despite interannual variation at each site, neither an increase nor a decrease in overall tree-ring width index was found, suggesting a lack of temperature related trend on radial growth for the time span (Figure 2A1–F1). An interannual variation was smaller on the

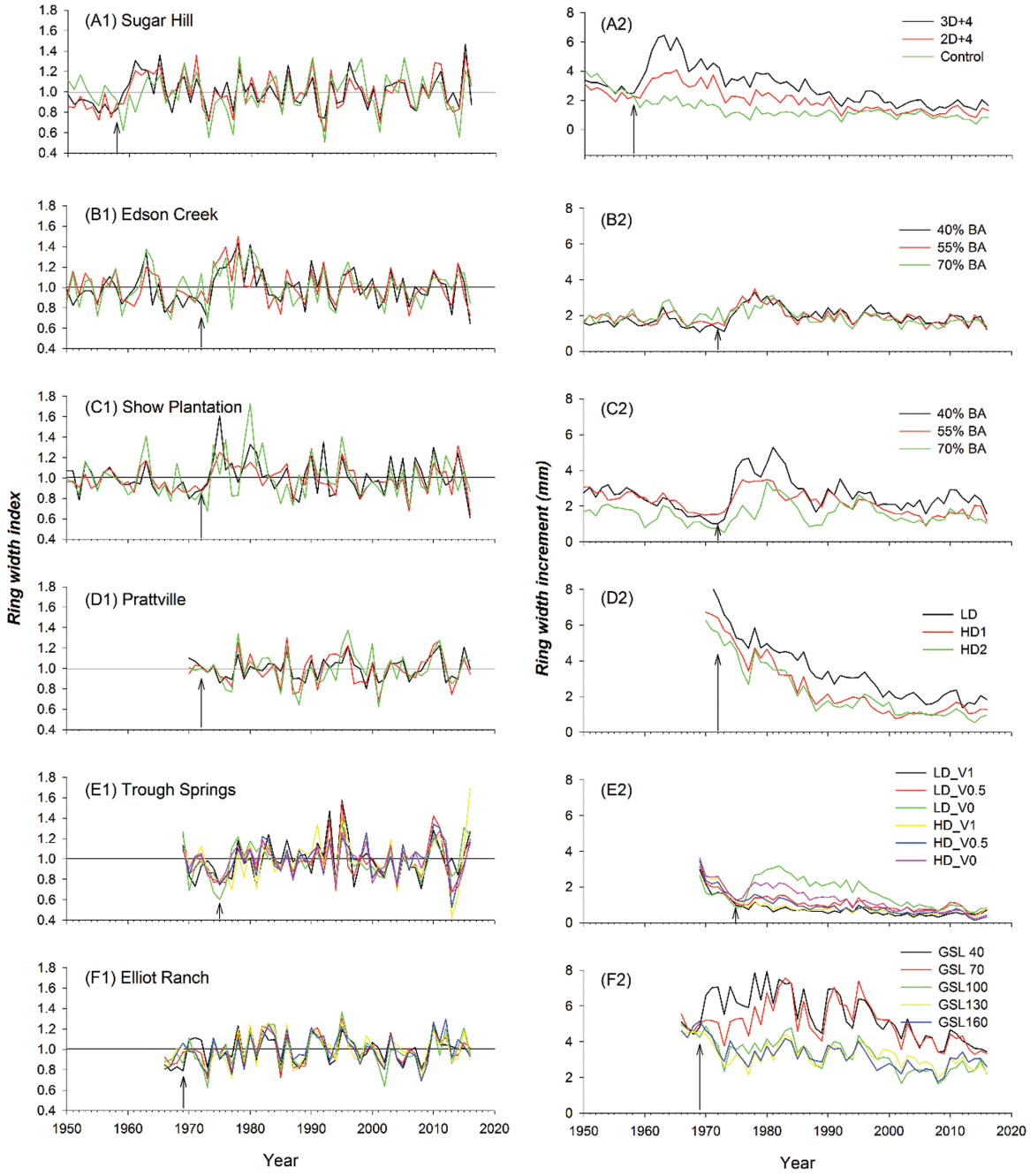

Figure 2. Ring-width indices (A1–F1) and increment (A2–F2) at six permanent plot sites. Arrows refer to the year when plots were installed.

lower-density plots than on the higher-density plots based on the SD of chronologies at each site (Table 2).

Comparing with other individual climate variables, the CMI, although $r^2 \leq .37$, explained the most variation of tree-ring width indices at all sites except at Edson Creek and Show Plantation, where the maximum VPD explained the most variation (Table 2). The slopes were always positive for CMI and negative for VPD. At Elliot Ranch, including the GDD0 in the model provided a better fit and prediction.

None of the individual or derived climate variables from combinations of individual ones, i.e., maximum, minimum, mean air temperature, precipitation, or VPD could explain more variability of tree-ring width index than the CMI. Because of different time spans between sites, variation among sites, among densities, and among years, no common trends could be generalized when we use the seasonal variation of climatic variables.

Lower density stands showed an increased diameter growth of remaining trees after treatment implementation (Figure 2A2–F2). The heavier the thinning intensity, the longer the thinning effect lasted. Since thinning was conducted at an older age, the thinning effect was not obvious in the natural stand at Edson Creek (Figure 2B2).

Plot-Level Growth

Although stand diameter (QMD) responded to thinning significantly (Figure 3A2–F2), the responses of plot-level net annual BA increment (MAI) to density were not obvious within sites with the exception of abrupt reductions of annual increment caused by mortality, usually occurring in the higher-density plots (Figure 3A1–F1). Mortality in some years was so heavy that it caused the significant differences in the overall MAI and net BA among densities within some sites (Table 3). In addition, not only did initial BA vary among sites because of the different thinning intensities, but also the site effect was significant for net BA, BA mortality, and MAI BA. Within each site, all BA-related variables except for MAI differed among densities or treatments. Both the higher initial BA and plots with a higher competition intensity showed less net BA accumulation, although this depended on stand developmental stages. For example, all plots with >19 $m^2\ ha^{-1}$ (83 $ft^2\ ac^{-1}$) in initial BA at Edson Creek and Show revealed low net BA and high mortality, whereas at Trough Springs, all treatment plots with <2 $m^2\ ha^{-1}$ (9 $ft^2\ ac^{-1}$) initial BA had a low net BA, although the percentage increase was high because of the age of the plots at the time of treatment (Table 3).

Mortality

Since plot establishment, mortality from a combination of abiotic stresses (such as water, nutrients, and light) and biotic disturbances (such as bark beetle outbreaks) has occurred mainly in higher-density plots at each site (Table 3). The zero-inflated binomial models showed that the model with SDI only is the best-performing model with LOO of 2311.73 (Table 4). The effect of SDI on the log odds of tree mortality is 0.009. This means that if SDI increases, the probability of mortality increases. The effect of CMI in the second best and third best model is negative and close to zero, implying that the probability of mortality decreases as CMI increases. However, the effect is small with a large credible interval and so probably close to zero provided that CMI is the climatic variable that influenced tree growth at most sites (Table 2). The log odds of zero-inflation is about 1.75 for all models, corresponding to a zero-inflated probability of 0.85 that no mortality will occur. This is in line with the 86 percent of observations experiencing no mortality. This 1 percent absolute difference in tree mortality could be attributed to misclassification of dead trees, although it is within the margin of error.

Figure 4 contains a scatterplot of the proportion of tree mortality by SDI. We can see the increasing trend in mortality over SDI from the binomial part of the model. Note that if the fits were corrected for the zero-inflation probability, the model would fit very close to zero for all SDI values. This is due to the very high amount of zero-inflation prevalent in this dataset.

Although attributing CMI to mortality was overwhelmed by SDI in the model, the climate effect on mortality cannot be ignored because a major mortality event was often parallel to or following a dry spell from multiple drought years. The phenomena were demonstrated at Elliot Ranch representing the best site quality (Figure S3) and at Sugar Hill as a lower site quality (Figures S4). Nonetheless, very few or no trees died in the lower-density plots during these dry spells.

Discussion

The detailed tracking records for these long-term ponderosa pine research plots demonstrated that lowering stand density enhanced remaining tree growth (Table 3; Figure 2), reduced mortality (Table 3; Figures 3 and 4), and increased stand resiliency to disturbance (Figure 3A2–F2) and climate change (Table 2; Figure 2A1–F1) reflected by the lower variability within the lower-density plots than in the higher-density plots. The results have been consistent with the results in previous studies, although very few have simultaneously examined these effects. Obviously, lowering density may not be a sole practice to improve forest health and resiliency. Any treatment that reduces tree stress will have a positive effect on stand-level health (i.e., less mortality) and individual tree-level growth. An example of an additional treatment demonstrated in this paper was the removal of competing understory shrubs at Trough Springs (Figure 2E1–E2). Favorable climate conditions such as higher CMI or lower VPD can reduce tree stress as well and improve resilience (Table 2). These results should not be surprising because an onset of self-thinning of ponderosa pine stands occurs at relatively lower SDI than of other sympatric species (Zhang et al. 2013a). In addition, growth rate could have been rapid under high-quality site conditions such as at Elliot Ranch. Therefore, intertree competition begins early for water, nutrients, and light, which makes trees grow under greater stress (Zhang et al. 2006). Furthermore, these crowded stands are more vulnerable to wildfires and outbreaks of pests and pathogens (Agee and Skinner 2005, Fettig et al. 2007). To mitigate these threats, one should consider stand density management and prescribed fire in both young and old stands (Stephens et al. 2012).

Climate Change and Forest Growth

Over the last 65 years, although climatic warming occurred at these study sites (Figure S1), a corresponding long-term trend of ponderosa pine growth was not detected (Figure 2A1–F1). The results differed from the findings recently reported that forest growth tracked a long-term climate trend by either increased or decreased growth. Studying the oldest research plots for Norway

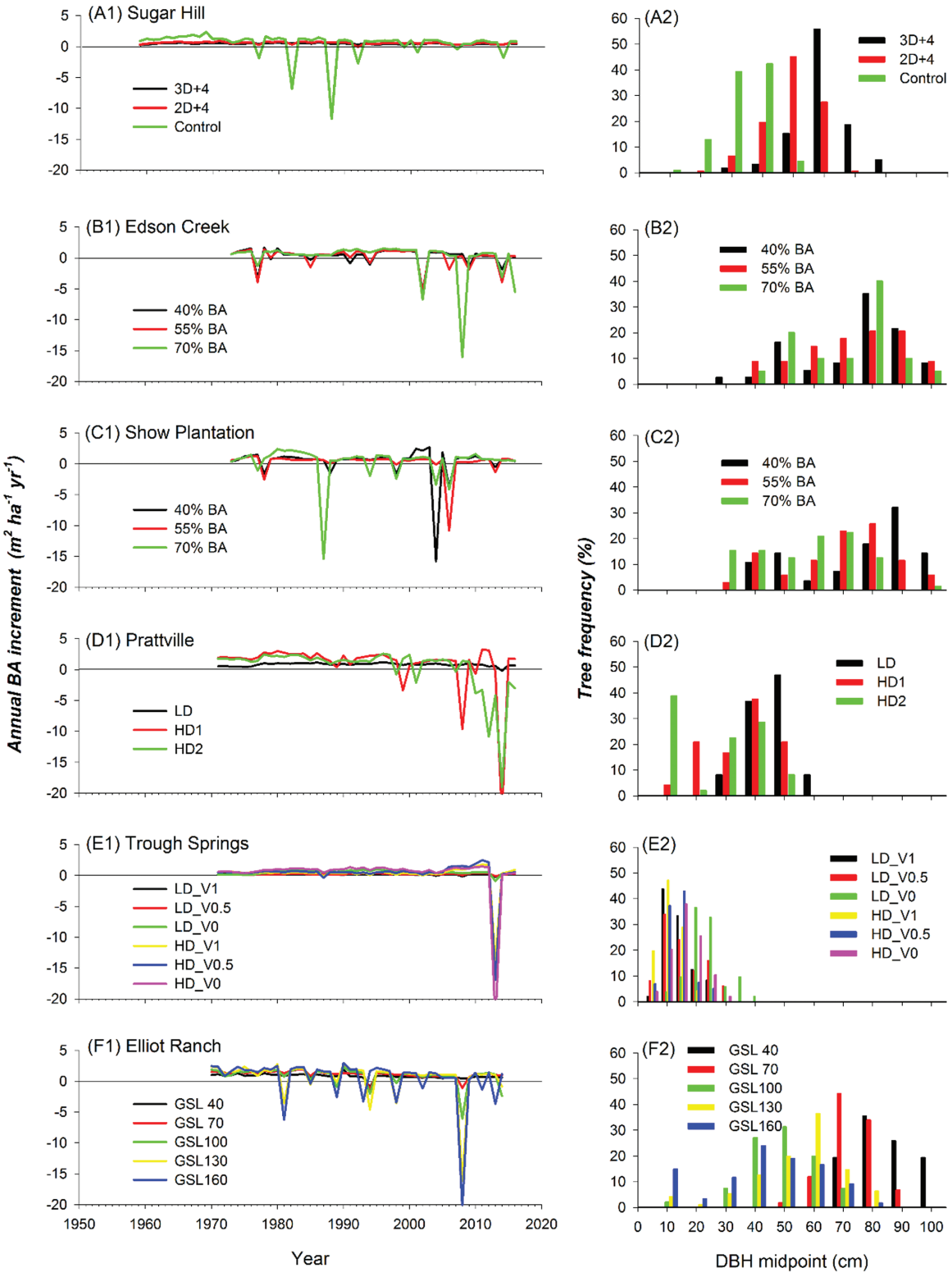

Figure 3. Annual basal area increment since research plots were installed and dbh distribution on the latest measurements for ponderosa pine grown in the northern California.

spruce (*Picea abies* [L.] Karst.) and European beech (*Fagus sylvatica* L.) in Central Europe, Pretzsch et al. (2014) found significantly faster tree growth today than in 1960, mainly because of increasing temperature and extended growing seasons. The growth acceleration was more obvious on fertile sites. Bristlecone pine (*Pinus longaeva* D.K. Bailey) showed the similar growth surge within 150 m of the upper tree line in the Great Basin, which was related to increased temperature in the second half of the 20th century (Salzer et al. 2009). Silva et al. (2016) reported that a synergistic effect of warming climate and the rise of CO_2 not only increased growth of *Abies faxoniana* Rehder & E.H.Wilson, but also accelerated the expansion of alpine forests in the Tibetan

Table 3. Study duration, initial TPH and BA after density treatments were established, net BA growth including further thinned trees, mortality, and MAI since these research plots were installed for ponderosa pine grown at various treatments in northern California.

Site	Study duration (years)	Treatment	Initial TPH	Initial BA (m^2 ha^{-1})	Net BA (m^2 ha^{-1})	Mortality (m^2 ha^{-1})	MAI (m^2 ha^{-1} $year^{-1}$)
Sugar Hill	62	3*D*+4	105	2.95	27.51	0.00	0.48
		2*D*+4	200	5.68	32.92	0.05	0.57
		Control	1,127	17.17	29.00	26.34	0.51
Edson Creek	44	40%BA	163	27.32	12.95	14.60	0.30
		55%BA	166	29.27	8.47	19.61	0.18
		70%BA	198	37.70	2.07	32.74	0.05
Show Plantation	44	40%BA	175	19.49	13.57	24.91	0.30
		55%BA	148	23.72	11.04	14.95	0.25
		70%BA	385	34.90	13.45	28.36	0.30
Prattville	45	LD	100	9.84	37.24	0.21	0.80
		HD1	1,070	13.79	12.81	49.48	0.28
		HD2	949	18.59	41.17	37.65	0.90
Trough Springs	46	LD_V1	556	0.76	7.14	0.48	0.16
		LD_V0.5	536	0.55	9.53	0.14	0.21
		LD_V0	576	0.51	22.64	0.90	0.48
		HD_V1	2,135	1.52	10.42	13.87	0.23
		HD_V0.5	2,135	1.79	13.68	17.29	0.30
		HD_V0	1,984	1.77	15.96	23.51	0.34
Elliot Ranch	45	GSL40	190	8.77	36.30	0.94	0.80
		GSL70	393	14.79	50.17	2.36	1.13
		GSL100	610	20.83	40.98	11.73	0.92
		GSL130	855	26.95	28.70	29.43	0.64
		GSL160	1,253	33.20	16.69	42.57	0.37

Note: BA, basal area; MAI, mean annual increment; TPH, trees per hectare

Table 4. Estimates of the binomial model intercept, zero-inflated model intercept, the effect of CMI and SDI, the respective 95 percent CIs, and the estimated LOO.

Model	β_0	β_0 CI	β_z	β_z CI	β_{cmi}	β_{cmi} CI	β_{sdi}	β_{sdi} CI	LOO
SDI	–5.13	(–5.31, –4.94)	1.73	(1.52, 1.94)	[a]	[a]	0.009	(0.008, 0.009)	2,311.73
CMI	–3.20	(–3.33, –3.06)	1.77	(1.6, 1.96)	–0.03	(–0.15, 0.09)	[a]	[a]	3,120.04
SDI, CMI	–5.02	(–5.21, –4.82)	1.70	(1.52, 1.89)	–0.12	(–0.24, –0.01)	0.009	(0.008, 0.009)	2,316.47

Note: [a]Term not included in a model. CI, credible interval; CMI, Climatic Moisture Index; LOO, Leave One Out Information Criterion; SDI, Stand Density Index

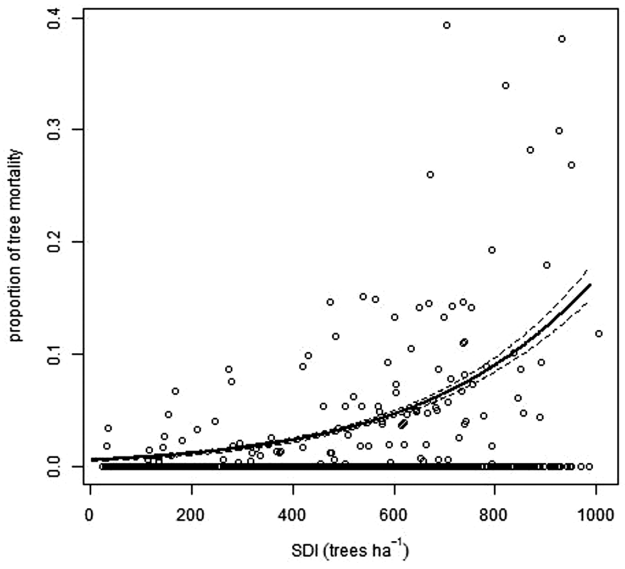

Figure 4. Scatterplot of proportion of annual tree mortality by SDI. The solid line is the posterior mean fit of the expected proportion of tree mortality from binomial part of model 1. Dashed lines are a 95 percent credible interval for the fit.

Plateau. Using a dataset of tree biomass from 55 temperate forest plots, McMahon et al. (2010) reported a recent increase in forest growth that was hypothesized to relate to increased temperature, growing season, and/or CO_2, nutrient fertilization, community composition, and demographic stochasticity. In ponderosa pine, the long-term negative or no growth trends were found in Northern Arizona from 1920 to 1990, which was consistent with the lack of trends for climatic variables (Biondi 1999). The lack of growth trends (neither negative nor positive) following temperature increases in these ponderosa pine stands might be related to tree adaptation to Mediterranean climate. We have found that the duration of the growing season was controlled by both temperature and soil water availability (unpublished data). Temperature determines a beginning of growing season, whereas it is soil water that determines growth duration and rate of tree growth unless there is abundant water in the soils. At Edson Creek and Show Plantation, soils are characterized as the Sadie, deep-Germany families association (150 cm or 59 in. depth) with high water-holding capacity. In addition, water from Mt. Shasta glaciers also provides soil water over the dry seasons during certain extremely hot years (personal observations). Therefore, it is no surprise that radial growth was more related to VPD than CMI as at other sites (Table 2). Other possible reasons for the difference in radial growth relation to climate at these locations are that they are the oldest trees in our study grown either in plantation at Show or in natural stand at Edson, where the EPS values were the lowest for all sites. Finally, to truly compare radial growth relations with climate between the different study locations, we would have to look at the same time spans for all studies.

Although there was no long-term growth trend for these stands across these years, radial growth responded to annual climate significantly, which has been indicated by interannual variations (Figure 2A1–F1). The effects of age and/or density manipulation were clearly demonstrated with tree-ring increment, i.e., age-related decline and release after thinning (Figure 2A2–F2), suggesting that long-term climate tracking for stand or tree growth would not be possible without the detrended series of tree cores.

Stand Density Manipulation and Forest Growth

The effect of stand density on tree growth has confirmed a widely observed principle that stands managed at lower densities grow larger-diameter trees (Figures 2A2–F2; 3A2–F2). This result is consistent with many previous studies regardless of tree species. The magnitude of growth response to stand density varied with site quality, stand origin, and stand ages (Figure 2). Significantly higher-diameter growth in lower-density stands indicates two benefits. First, large-diameter trees with a high proportion of carbon in the stem represent a more stable form of carbon storage than smaller-diameter trees if understory vegetation is similar (Zhang et al. 2010, North and Hurteau 2011, Earles et al. 2014). Furthermore, we cannot account for a complete forest carbon pool without considering wildfires in fire-dominated ecosystems (Powers 2010, Zhang et al. 2010). Ponderosa pine grown under the Mediterranean climate is surely such a system where larger-diameter trees grown in lower densities are typically better able to survive a fire than smaller trees (Agee and Skinner 2005). For example, a recent wildfire in the spring of 2018 that burnt through one of the lower-density plots at Elliot Ranch did not kill a single tree. This personal observation suggests that this particular lower-density plot may provide a more secure condition for carbon storage than the high-density plots.

Second, if the management goal is to produce large trees characteristic of late-seral forests, low-density stands are preferred. Management guidelines for late-seral forests on the east slope of the Cascade Range in Oregon and Washington included trees with a dbh of 53 cm (21 in.) (Youngblood et al. 2004), and in the Sierra Nevada trees with a dbh of 76 cm (30 in.) (cf. Zhang et al. 2013b). Many trees on our lower-density plots at high site quality have already grown to these size categories (Figure 3A2–F2).

At the stand level, the nonsignificant net annual growth for BA was surprising (Figure 3A1–F1). In general, we often found that high-density plots showed a higher annual BA growth (Daniel et al. 1979). Under a timber-management objective, the maximum site productivity is sustained by managing an optimal stand density that allows leaf area to reach its highest level (Pretzsch 2010). In this study, because mortality often occurred in those higher-density plots, net stand growth was either comparable or higher at lower-density plots than higher plots.

Stand Density and Mortality

Because yearly estimates were obtained for each plot, one might be interested in determining if there is a site or plot effect. Unfortunately, some sites did not include replications, and the distribution of SDI and CMI is not uniform across sites and plots. Thus, the effect of SDI and CMI is confounded with site and plot. Including site and plot in the model, as would be expected because of the number of parameters entailed, swamps out the effects of SDI and CMI, so they were not investigated as a part of this analysis. Nonetheless, the relation between SDI and mortality has been demonstrated in many studies for different species including ponderosa pine (Long and Shaw 2005, Zhang et al. 2013a, c). In ponderosa pine stands throughout western North America, several *Dendroctonus* species are not only important ecosystem components (Furniss and Carolin 1977), but also regarded as ubiquitous regulators of density in young, even-aged stands of ponderosa pine (Sartwell and Stevens 1975), although their periodic outbreaks with drought have the potential to cause widespread mortality of older trees in mature forests within large areas (Stephens et al. 2018). By analyzing 155 permanent plots in even-aged ponderosa pine stands in California, Oliver (1995) found that self-thinning started when SDI reached about 600 trees ha^{-1} (240 trees ac^{-1}), and significant mortality occurred when SDI reached about 900 trees ha^{-1} (365 trees ac^{-1}). This value was considerably below the maximum SDI of 1,060–1,236 trees ha^{-1} (429–500 trees ac^{-1}) used by foresters in the Western United States. However, Oliver (1995) argued that a limiting SDI of 900 trees ha^{-1} (365 trees ac^{-1}) is the result of increased bark beetle activity. Our study here indicated an increasing trend of mortality with SDI, which is shown by the fitted line from the rather large variation of mortality at a specific SDI (Figure 4). For example, it reached about 5 percent mortality rate yearly when the SDI was 600 trees ha^{-1} (240 trees ac^{-1}), although a maximum of 15 percent mortality rate could occur on some plots at certain sites. Similarly, a model prediction for mortality reached 12 percent when the SDI was 900 trees ha^{-1} (365 trees ac^{-1}), but we observed that a maximum rate of mortality could reach as high as 40 percent when SDI was 700 trees ha^{-1} (283 trees ac^{-1}). Therefore, for all disturbances considered, it appears that the original limiting SDI should have been lower in this region.

It may be possible to improve upon the choice of binomial in the zero-inflated binomial. This choice, while well motivated, was also partly influenced by what was available in software at the time of this analysis. It may be that a model that allows for overdispersion, such as the betabinomial model, would be appropriate for modeling our uncertainty in tree mortality. This would also account for dependence in mortality among individual trees within year within plot. Indeed, a model that allows for more variability may fix the issues we experienced in computing LOO by broadening the range of negligible points.

Climate Change and Disturbances

Although the effect of climate change on a suite of disturbances is beyond the scope of this study, we did find that most mortality events, especially those heavy ones, were often parallel to or following a dry spell from multiple drought years (Figures S3–S4). The results are consistent with findings from many previous studies during recent years (e.g., Allen et al. 2010, Bradford and Bell 2017). These studies and comprehensive reviews demonstrated that the massive mortality could have been caused by severe droughts or drought-related bark beetle outbreaks such as in the mixed conifer forests in the Sierra Nevada of California (Stephens et al. 2018), but also provided the mechanistic processes of tree mortality from droughts (Choat et al. 2018). Seidl et al. (2017) found that more than 70 percent of droughts were directly caused by climate change with increasing temperature and decreasing precipitation. In addition, climate change also affects many other disturbances

such as climate warming increasing wildfire frequency and severity (Westerling et al. 2006) and causing species extinctions worldwide (Thomas et al. 2004). Practically, forest managers cannot control both climate and disturbances, but what they can do is to manage stand density based on stand age and environmental conditions to mitigate the threats from climate change and potential disturbances.

Conclusions

Using a dendrochronological approach and frequent inventories for permanent research plots, we found that regardless of site quality, reducing stand density increased the diameter growth of residual trees, reduced stand mortality, and enhanced stand resiliency to disturbance and climate change. Any treatments that released trees' stress would have a positive effect on stand-level health (lower mortality rate) and individual tree-level growth, as would favorable climate conditions such as a higher climate moisture index or lower VPD. Although annual temperature has gradually increased at all sites for the last 65 years, tree-ring indices, which eliminate age and thinning effects, failed to reflect a long-term radial growth trend at any site. However, the high volatility in ring-width suggests a strong influence of climate on tree growth. Plot-level BA increments were significantly affected by tree mortality. SDI explained most variation of mortality because very few or no trees had died in the lower-density plots since plot establishment. Since neither biotic disturbances nor abiotic conditions can be controlled, forest managers can manage forest stands with an appropriate stand density to avoid abnormal consequences caused by climate change and the potential disturbances.

Literature Cited

Agee, J.K., and C.N. Skinner. 2005. Basic principles of forest fuel reduction treatments. *For. Ecol. Manage.* 211:83–96.

Allen, C.D., A.K. Macalady, H. Chenchouni, D. Bachelet, N. McDowell, M. Vennetier, T. Kitzbergerg, et al. 2010. A global overview of drought and heat-induced tree mortality reveals emerging climate change risks for forests. *For. Ecol. Manage.* 259:660–684.

Baker, P.J., J.G. Palmer, and R. D'Arrigo. 2008. The dendrochronology of *Callitris intratropica* in northern Australia: Annual ring structure, chronology development and climate correlations. *Aust. J. Bot.* 56:311–320.

Buras, A. 2017. A comment on the expressed population signal. *Dendrochronologia* 44:130–132.

Biondi, F. 1999. Comparing tree-ring chronologies and repeated timber inventories as forest monitoring tools. *Ecol. Appl.* 9(1):216–227.

Bonan, G.B. 2008. Forests and climate change: Forcings, feedbacks, and the climate benefits of forests. *Science* 320:1444–1449.

Bradford, J.B., and D.M. Bell. 2017. A window of opportunity for climate-change adaptation: Easing tree mortality by reducing forest basal area. *Front Ecol. Environ.* 15(1):11–17.

Bürkner, P.-C. 2017. brms: An R package for Bayesian multilevel models using stan. *J. Stat. Softw.* 80(1):1–28.

Choat, B., T.J. Brodribb, C.R. Brodersen, R.A. Duursma, R. Lopez, and B.E. Medlyn. 2018. Triggers of tree mortality under drought. *Nature* 558:531–539.

Cook, E.R. 1985. *A time series analysis approach to tree-ring standardization*. University of Arizona, Tucson, AZ.

Cook, E.R., and R.L. Holmes. 1999. *User's manual for program ARSTAN*. Laboratory of Tree-Ring Research, University of Arizona, Tucson, AZ.

Daly, C., M. Halbleib, J.I. Smith, W.P. Gibson, M.K. Doggett, G.H. Taylor, J. Curtis, and P.P. Pasteris. 2008. Physiographically sensitive mapping of climatological temperature and precipitation across the conterminous United States. *Int. J. Climatol.* 28:2031–2064.

Daniel, T.W., J.A. Helms, and F.S. Baker. 1979. *Principles of silviculture*. McGraw-Hill, New York.

Duane, S., A.D. Kennedy, B.J. Pendleton, and D. Roweth. 1987. Hybrid Monte Carlo. *Phys. Lett. B* 195(2):216–222.

Earles, J.M., M.P. North, and M.D. Hurteau. 2014. Wildfire and drought dynamics destabilize carbon stores of fire-suppressed forests. *Ecol. Appl.* 24(4):732–740.

Fettig, C.J., K.D. Klepzig, R.F. Billings, A.S. Munson, T.E. Nebeker, J.F. Negron, and J.T. Nowak. 2007. The effectiveness of vegetation management practices for prevention and control of bark beetle outbreaks in coniferous forests of the western and southern United States. *For. Ecol. Manage.* 238:24–53.

Fritts, H.C., and T.W. Swetnam. 1989. Dendroecology: A tool for evaluating variations in past and present forest environments. *Adv. Ecol. Res.* 19:111–188.

Furniss, R.L., and V.M. Carolin. 1977. *Western forest insects*. USDA Forest Service, Misc. Publ. 1339, Washington DC. 654 p.

Gelman, A., J.B. Carlin, H.S. Stern, D.B. Dunson, A. Vehtari, and D.B. Rubin. 2013. *Bayesian data analysis*. 3rd ed. Chapman & Hall/CRC, Boca Raton, FL.

Grissino-Mayer, H.D. 2001. Evaluating crossdating accuracy: A manual and tutorial for the computer program COFECHA. *Tree Ring Res.* 57:205–221.

Hall, D.B. 2000. Zero-Inflated poisson and binomial regression with random effects: A case study. *Biometrics* 56:1030–1039.

Hoffman, M.D., and A. Gelman. 2014. The No-U-turn sampler: Adaptively setting path lengths in Hamiltonian Monte Carlo. *J. Mach. Learn Res.* 15(1):1593–1623.

IPCC. 2014. *Fifth assessment report*. Cambridge University Press, Cambridge.

Long, J.N., and J.D. Shaw. 2005. A density management diagram for even-aged ponderosa pine stands. *West. J. Appl. For.* 20:205–215.

Lugo, A.E. 2015. Forestry in the anthropocene. *Science* 349:771.

McDowell, N.G., H.A. Adams, J.D. Bailey, M. Hess, and T.E. Kolb. 2006. Homeostatic maintenance of ponderosa pine gas exchange in response to stand density changes. *Ecol. Appl.* 16:1164–1182.

McDowell, N.G., J.R. Brooks, S. Fitzgerald, and B.J. Bond. 2003. Carbon isotope discrimination and growth response of old ponderosa pine trees to stand density reductions. *Plant. Cell. Environ.* 26:631–644.

McMahon, S.M., G.G. Parker, and D.R. Miller. 2010. Evidence for a recent increase in forest growth. *Proc. Natl. Acad. Sci. USA* 107:3611–3615.

Meyer, W.H. 1938. *Yield of even-aged stands of ponderosa pine*. USDA Tech. Bull. No. 63, Washington, DC. 59 p.

North, M.P., and M.D. Hurteau. 2011. High-severity wildfire effects on carbon stocks and emissions in fuels treated and untreated forest. *For. Ecol. Manage.* 261:1115–1120.

Oliver, W.W. 1995. Is self-thinning of ponderosa pine ruled by *Dendroctonus* bark beetle? P. 213–218 in *Forest health through silviculture: Proceedings of the National Silviculture Workshop: 1995 May 8–11*, L.G. Eskew (comp.). USDA Forest Service, Gen. Tech. Rep. RM-GTR-267, Mescalero, NM.

Oliver, W.W., and R.F. Powers. 1978. *Growth models for ponderosa pine. I: Yield of unthinned plantations in northern California*. USDA Forest Service, Res. Pap. PWS-133, Berkeley, CA. 21 p.

Powers, R.F. 2010. Carbon opportunity lost in unmanaged forests. *Calif. For.* 14:12–13.

Pretzsch, H. 2010. *Forest dynamics, growth and yield*. Springer, Berlin, Germany. 664 p.

Pretzsch, H., P. Biber, G. Schutze, E. Uhl, and T. Rotzer. 2014. Forest stand growth dynamics in Central Europe have accelerated since 1870. *Nature Comm.* 5:4967.

R Core Team. 2017. *R: A language and environment for statistical computing*. R Foundation for Statistical Computing, Vienna, Austria. Available online at https://www.R-project.org/; last accessed April 3, 2018.

Reineke, L.H. 1933. Perfecting a stand-density index for even-aged forests. *J. Agri. Res.* 46:627–638.

Ritchie, M.W., J.W. Zhang, and T. Hamilton. 2012. Effects of stand density on top height estimation for ponderosa pine. *West. J. Appl. For.* 27(1):18–24.

Salzer, M.W., M.K. Hughes, A.G. Bunn, and K.F. Kipfmueller. 2009. Recent unprecedented tree-ring growth in bristlecone pine at the highest elevations and possible causes. *Proc. Natl. Acad. Sci. USA* 106:20348–20353.

Sartwell, C., and R.E. Stevens. 1975. Mountain pine beetle in ponderosa pine—Prospects for silvicultural control in second growth stands. *J. For.* 73(3):136–140.

Schwab, N., R.J. Kaczka, K. Janecka, J. Bohner, R.P. Chaudhary, T. Scholten, and U. Schickhoff. 2018. Climate change-induced shift of tree growth sensitivity at a central Himalayan treeline ecotone. *Forests* 9:267.

Seidl, R., D. Thom, M. Kautz, D. Martin-Benito, M. Peltoniemi, G. Vacchiano, J. Wild, et al. 2017. Forest disturbances under climate change. *Nat. Clim. Change* 7:395–402.

Silva, L.C.R., G. Sun, X. Zhu-Barker, Q. Liang, N. Wu, and W.R. Horwath. 2016. Tree growth acceleration and expansion of alpine forests: The synergistic effect of atmospheric and edaphic change. *Sci. Adv.* 2(8):e1501302.

Sohn, J.A., T. Gebhardt, C. Ammer, J. Bauhus, K.-H. Häberle, R. Matyssek, and T.E.E. Grams. 2013. Mitigation of drought by thinning: Short-term and long-term effects on growth and physiological performance of Norway spruce (Piceaabies). *For. Ecol. Manage.* 308:188–197.

Sohn, J.A., F. Hartig, M. Kohler, J. Huss, and J. Bauhus. 2016a. Heavy and frequent thinning promotes drought adaptation in *Pinus sylvestris* forests. *Ecol. Appl.* 26:2190–2205.

Sohn, J.A., S. Saha, and J. Bauhus. 2016b. Potential of forest thinning to mitigate drought stress: A meta-analysis. *For. Ecol. Manage.* 380:261–273.

Speer, J.H. 2010. *Fundamentals of tree-ring research*. University of Arizona Press, Tucson, AZ.

Stan Development Team. 2017. The Stan Core Library, Version 2.17.0. Available online at http://mc-stan.org; last accessed April 3, 2018.

Stephens, S.L., J.D. McIver, R.E.J. Boerner, C.J. Fettig, J.B. Fontaine, B.R. Hartsough, P. Kennedy, and D.W. Schwilk. 2012. Effects of forest fuel reduction treatments in the United States. *BioScience* 62:549–560.

Stephens, S.L., B.M. Collins, C.J. Fettig, M.A. Finney, C.M. Hoffman, E.E. Knapp, M.P. North, H. Safford, and R. Wayman. 2018. Drought, tree mortality, and wildfire in forests adapted to frequent fire. *BioScience* 68(2):77–88.

Stokes, M.A., and T.L. Smiley. 1996. *An introduction to tree-ring dating*. The University of Arizona Press, Tucson, AZ.

Thomas, C.D., A. Cameron, R.E. Green, M. Bakkenes, L.J. Beaumont, Y.C. Collingham, B.F.N. Erasmus, et al. 2004. Extinction risk from climate change. *Nature* 427:145–148.

Trumbore, S., P. Brando, and H. Hartmann. 2015. Forest health and global change. *Science* 349:814–818.

Vehtari, A., A. Gelman, and J. Gabry. 2016a. Practical Bayesian model evaluation using leave-one-out cross-validation and WAIC. *Stat. Comput.* 27(5):1413–1432.

Vehtari, A., A. Gelman, and J. Gabry. 2016b. Pareto smoothed importance sampling. *arXiv.* Available online at http://arxiv.org/abs/1507.02646/; last accessed April 3, 2018.

Vitousek, P.M., H.A. Mooney, J. Lubchenco, and J.M. Melillo. 1997. Human domination of earth's ecosystems. *Science* 277:494–499.

Westerling, A.L., H.G. Hidalgo, D.R. Cayan, and T.W. Swetnam. 2006. Warming and earlier spring increase western U.S. forest wildfire activity. *Science* 313:940–943

Willmott, C.J., and J.J. Feddema. 1992. A more rational climatic moisture index. *Prof. Geogr.* 44(1):84–88.

Wigley, T.M.L., K.R. Briffa, and P.D. Jones. 1984. On the average value of correlated time series, with applications in dendroclimatology and hydrometeorology. *J. Clim. Appl. Meteorol.* 23:201–213.

Yamaguchi, D.K. 1991. A simple method for cross-dating increment cores from living trees. *Can. J. For. Res.* 21:414–416.

Youngblood, A., T. Max, and K. Coe. 2004. Stand structure in eastside old-growth ponderosa pine forests of Oregon and northern California. *For. Ecol. Manage.* 199:191–217.

Zhang, J.W., W.W. Oliver, and M.D. Busse. 2006. Growth and development of ponderosa pine on sites of contrasting productivities: Relative importance of stand density and shrub competition effects. *Can. J. For. Res.* 36:2426–2438.

Zhang, J.W., W.W. Oliver, and R.F. Powers. 2013a. Reevaluating the self-thinning boundary line for ponderosa pine (*Pinus ponderosa*) forests. *Can. J. For. Res.* 43:963–971.

Zhang, J.W., W.W. Oliver, M.W. Ritchie, and D.L. Neal. 2013b. Overstory and understory dynamics in a ponderosa pine plantation vary with stand density in the Sierra Nevada: 40-year results. *For. Sci.* 59(6):670–680.

Zhang, J.W., R.F. Powers, and C.N. Skinner. 2010. To manage or not to manage: The role of silviculture in sequestering carbon in the specter of climate change. P. 95–110 in *Integrated management of carbon sequestration and biomass utilization opportunities in a changing climate: Proceedings of the 2009 National Silviculture Workshop*, June 15–18, 2009, Jain, T.B., R.T. Graham, and J. Sandquist (tech. eds.). USDA Forest Service, RMRS-P-61, Boise, ID.

Zhang, J.W., M.W. Ritchie, D.A. Maguire, and W.W. Oliver. 2013c. Thinning ponderosa pine stands reduces mortality while maintaining stand productivity. *Can. J. For. Res.* 43:311–320.